DALTON
FULL PAPER

Ligand-stabilization of an unusual square-based pyramidal geometry of Cd(II) and Zn(II) in an heterometallic $\{MPt_2S_2\}$ core (M = Cd, Zn)

Zhaohui Li,[a] Zhi-Heng Loh,[a] S.-W. Audi Fong,[a] Yaw-Kai Yan,[b] William Henderson,[c] K. F. Mok[a]* and T. S. Andy Hor[a]*

[a] *Department of Chemistry, National University of Singapore, 3 Science Drive 3, Singapore 117543. E-mail: chmandyh@nus.edu.sg*
[b] *Division of Chemistry, National Institute of Education, Nanyang Technological University, 469 Bukit Timah Road, Singapore 259156*
[c] *Department of Chemistry, University of Waikato, Private Bag 3105, Hamilton, New Zealand*

Received 23rd November 1999, Accepted 8th February 2000

Two heterometallic complexes, $[Pt_2MCl(bipy)(PPh_3)_4(\mu_3\text{-}S)_2][PF_6]$ (M = Zn, **2**, Cd, **3**) were synthesized from $[Pt_2(PPh_3)_4(\mu\text{-}S)_2]$ and characterized by single-crystal X-ray diffraction and electrospray ionization mass spectrometry. Two unusual square-based pyramidal (sbp) Zn(II) and Cd(II) structures are evident. VT $^{31}P\text{-}\{^1H\}$ NMR studies showed that **2** and **3** are fluxional at rt whereby rapid ligand exchange takes place by a non-dissociative mechanism. At intermediate temperatures, this motion slows down to a flipping movement of the $\{Pt_2S_2\}$ ligand. At 183 K, all four phosphines are inequivalent in a distorted sbp model similar to that observed in the solid state. Nonlocal density functional theory calculations reveal that the formation of a trigonal bipyramidal intermediate in the fluxional process is favored over that of the tetrahedral species for both **2** and **3**. The M–Cl (M = Zn, Cd) bonds are notably strong.

Introduction

Current interest in the ligand environment of Zn(II) in DNA-binding proteins and zinc-based enzymes[1] has generated some significant activities in the study of the structures of Zn(II) complexes. Although Zn(II) is generally assumed to be tetra-coordinate in the resting state of the biological system, a reactive intermediate with five-coordinate Zn(II) has been proposed in the reversible hydration of CO_2 by carbonic anhydrase and in liver alcohol dehydrogenase.[2] Such coordination is known but rare. A recent review[3] cited over 600 Zn complexes which are predominantly tetrahedral. Among the less common five-coordinate complexes, trigonal bipyramidal (tbp) geometry occurs more frequently than square-based pyramidal (sbp). The latter case is usually sustained by a basal plane of the donor atoms in a tetradentate macrocycle, with the apical position occupied by a terminal ligand such as pyridine (py) or chloride, *e.g.* $Zn(tpc)(py)\cdot C_6H_6$ (H_2tpc = tetraphenylchlorin),[4] $[Zn(tmt)Cl][ClO_4]$ (tmt = 1,4,8,11-tetramethyl-1,4,8,11-tetraazacyclotetradecane)[5] and $[Zn(H_2L)Cl]Cl\cdot 2H_2O$ (H_2L = cyclohexane-1,2-dione bis(thiosemicarbazone)].[6] Compared to these, Cd(II) cationic complexes are generally found in six- and four-coordination while five-coordinate complexes are less common, *e.g.* $[CdI_2L]$[7] (L = 2,5,8,10,13,16-hexaazapentacyclo-[8.6.1.1.0.0]octadecane, $[(CdLCl_2)_2]$ (L = 3-amino-6,6′-dimethyl-2,2′-bipyridine)[8] and $[CdCl_3(thiamin)]_2\cdot 2H_2O$.[9] These examples include both tbp and sbp structures. We herein report the synthesis, structures and fluxionality of two novel five-coordinate Zn(II) and Cd(II) heterometallic complexes formed from the metalloligand $[Pt_2(PPh_3)_4(\mu\text{-}S)_2]$ (**1**). The use of the latter as an entry point to a multimetallic system has been established.[10] The stability of these complexes is further evaluated by nonlocal density functional theory (NLDFT) calculations.

Results and discussion

A mixture of **1**, $ZnCl_2$, and 2,2′-bipyridyl (bipy) in MeOH gives rise to $[Pt_2ZnCl(bipy)(PPh_3)_4(\mu_3\text{-}S)_2][PF_6]$ (**2**) after metathesis with NH_4PF_6. Single-crystal X-ray crystallographic analysis showed a sulfide-bicapped heterometallic $\{Pt_2Zn\}$ triangle with phosphines on Pt and the other ligands on Zn (Fig. 1 and Table 1). There are two crystallographically independent molecules (A and B) per unit cell with largely similar structural data. With both metals in their normal oxidation states, no direct M–M bond is envisaged (mean Pt···Pt 3.251 Å, Pt···Zn 3.204 Å). The local geometry at the Zn(II) atom is sbp with the chelating metalloligand and bipy ligands on the basal plane; the metal is displaced by 0.52 Å from the least-squares plane towards the apical chloride. Both Zn–N (mean 2.180(7) Å) and Zn–S (mean 2.494(2) Å) bonds are longer, and presumably weaker, than those in similar complexes *e.g.* $[Zn\{Ph(SCH_3)C{=}C(S)Ph\}_2(bipy)]$ (sbp)[11] (mean Zn–N 2.097(8) Å and Zn–S 2.283(3) Å), $[Zn(H_2L)Cl]Cl\cdot 2H_2O$ (sbp) (mean Zn–S 2.327 Å). The two Zn–S bonds in either independent molecule are signifi-

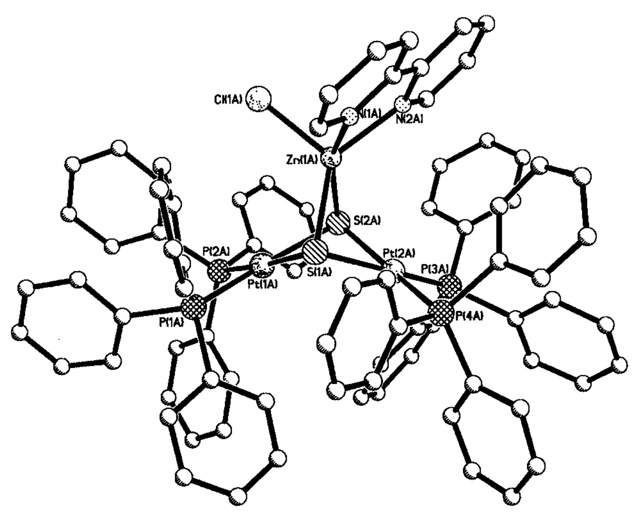

Fig. 1 Molecular structure of one of the two crystallographically independent molecules (A) of $[Pt_2ZnCl(bipy)(PPh_3)_4(\mu_3\text{-}S)_2]^+$ (**2**).

DOI: 10.1039/a909254d

Table 1 Selected bond lengths (Å) and bond angles (°) for $[Pt_2ZnCl(bipy)(PPh_3)_4(\mu_3\text{-}S)_2]^+$ (**2**) and $[Pt_2CdCl(bipy)(PPh_3)_4(\mu_3\text{-}S)_2]^+$ (**3**)

$[Pt_2ZnCl(bipy)(PPh_3)_4(\mu_3\text{-}S)_2][PF_6]$ (**2**)				$[Pt_2CdCl(bipy)(PPh_3)_4(\mu_3\text{-}S)_2][PF_6]$ (**3**)			
Molecule A							
Pt(1A)–P(1A)	2.299(2)	Pt(1A)–P(2A)	2.287(1)	Pt(1A)–P(1A)	2.292(2)	Pt(1A)–P(2A)	2.282(2)
Pt(1A)–S(1A)	2.362(2)	Pt(1A)–S(2A)	2.359(2)	Pt(1A)–S(1A)	2.359(2)	Pt(1A)–S(2A)	2.353(2)
Pt(2A)–P(3A)	2.316(2)	Pt(2A)–P(4A)	2.312(2)	Pt(2A)–P(3A)	2.308(2)	Pt(2A)–P(4A)	2.295(2)
Pt(2A)–S(1A)	2.357(2)	Pt(2A)–S(2A)	2.378(2)	Pt(2A)–S(1A)	2.353(2)	Pt(2A)–S(2A)	2.373(2)
Zn(1A)–N(1A)	2.209(7)	Zn(1A)–N(2A)	2.171(7)	Cd(1A)–N(1A)	2.374(6)	Cd(1A)–N(2A)	2.374(6)
Zn(1A)–S(1A)	2.450(2)	Zn(1A)–S(2A)	2.533(2)	Cd(1A)–S(1A)	2.627(2)	Cd(1A)–S(2A)	2.625(2)
Zn(1A)–Cl(1A)	2.299(2)	Pt(2A)···Zn(1A)	3.149(1)	Cd(1A)–Cl(1A)	2.468(2)	P1(1A)···Cd(1A)	3.314(1)
Pt(1A)···Pt(2B)	3.252(2)	Pt(1A)···Zn(1A)	3.260(1)	Pt(2A)···Cd(1A)	3.226(1)	Pt(1A)···Pt(2A)	3.274(3)
Molecule B							
Pt(1B)–P(1B)	2.283(2)	Pt(1B)–P(2B)	2.306(2)	Pt(1B)–P(1B)	2.305(2)	Pt(1B)–P(2B)	2.295(2)
Pt(1B)–S(1B)	2.354(2)	Pt(1B)–S(2B)	2.366(2)	Pt(1B)–S(1B)	2.373(2)	Pt(1B)–S(2B)	2.349(2)
Pt(2B)–P(3B)	2.311(2)	Pt(2B)–P(4B)	2.311(2)	Pt(2B)–P(3B)	2.298(2)	Pt(2B)–P(4B)	2.272(2)
Pt(2B)–S(1B)	2.377(2)	Pt(2B)–S(2B)	2.356(2)	Pt(2B)–S(1B)	2.353(2)	Pt(2B)–S(2B)	2.364(2)
Zn(1B)–N(1B)	2.144(7)	Zn(1B)–N(2B)	2.194(7)	Cd(1B)–N(1B)	2.390(6)	Cd(1B)–N(2B)	2.342(6)
Zn(1B)–S(1B)	2.565(2)	Zn(1B)–S(2B)	2.426(2)	Cd(1B)–S(1B)	2.656(2)	Cd(1B)–S(2B)	2.586(2)
Zn(1B)–Cl(1B)	2.283(2)	Pt(2B)···Zn(1B)	3.139(1)	Cd(1B)–Cl(1B)	2.444(2)	Pt(1B)···Cd(1B)	3.266(1)
Pt(1B)···Pt(2B)	3.249(2)	Pt(1B)···Zn(1B)	3.266(1)	Pt(2B)···Cd(1B)	3.274(1)	Pt(1B)···Pt(2B)	3.257(3)
Molecule A							
P(1A)–Pt(1A)–S(1A)	87.10(7)	P(1A)–Pt(1A)–S(2A)	167.45(7)	P(1A)–Pt(1A)–S(1A)	86.12(6)	P(1A)–Pt(1A)–S(2A)	168.02(6)
P(2A)–Pt(1A)–S(1A)	174.45(7)	P(2A)–Pt(1A)–S(2A)	94.62(7)	P(2A)–Pt(1A)–S(1A)	175.22(6)	P(2A)–Pt(1A)–S(2A)	93.60(6)
P(2A)–Pt(1A)–P(1A)	97.92(7)	S(2A)–Pt(1A)–S(1A)	80.35(6)	P(2A)–Pt(1A)–P(1A)	98.36(6)	S(2A)–Pt(1A)–S(1A)	81.91(5)
P(3A)–Pt(2A)–S(1A)	166.52(7)	P(3A)–Pt(2A)–S(2A)	87.42(7)	P(3A)–Pt(2A)–S(1A)	167.00(6)	P(3A)–Pt(2A)–S(2A)	86.38(6)
P(4A)–Pt(2A)–P(3A)	103.18(8)	P(4A)–Pt(2A)–S(2A)	168.68(8)	P(4A)–Pt(2A)–P(3A)	102.83(7)	P(4A)–Pt(2A)–S(2A)	170.30(6)
P(4A)–Pt(2A)–S(1A)	89.68(7)	S(1A)–Pt(2A)–S(2A)	80.08(6)	P(4A)–Pt(2A)–S(1A)	89.45(6)	S(1A)–Pt(2A)–S(2A)	81.62(5)
N(1A)–Zn(1A)–S(1A)	92.0(2)	N(1A)–Zn(1A)–S(2A)	158.6(2)	N(1A)–Cd(1A)–S(1A)	92.72(17)	N(1A)–Cd(1A)–S(2A)	155.53(18)
N(2A)–Zn(1A)–S(1A)	134.2(2)	N(2A)–Zn(1A)–S(2A)	102.2(2)	N(2A)–Cd(1A)–S(1A)	131.69(16)	N(2A)–Cd(1A)–S(2A)	107.09(16)
N(1A)–Zn(1A)–Cl(1A)	95.7(2)	N(2A)–Zn(1A)–Cl(1A)	103.4(2)	N(1A)–Cd(1A)–Cl(1A)	94.91(18)	N(2A)–Cd(1A)–Cl(1A)	104.28(16)
N(2A)–Zn(1A)–N(1A)	74.1(3)	S(1A)–Zn(1A)–S(2A)	75.35(7)	N(2A)–Cd(1A)–N(1A)	68.5(2)	S(1A)–Cd(1A)–S(2A)	72.05(5)
Cl(1A)–Zn(1A)–S(1A)	121.50(8)	Cl(1A)–Zn(1A)–S(2A)	105.69(8)	Cl(1A)–Cd(1A)–S(1A)	121.93(6)	Cl(1A)–Cd(1A)–S(2A)	109.35(6)
Molecule B							
P(1B)–Pt(1B)–S(1B)	93.46(7)	P(1B)–Pt(1B)–S(2B)	173.32(7)	P(1B)–Pt(1B)–S(1B)	87.85(6)	P(1B)–Pt(1B)–S(2B)	168.47(6)
P(2B)–Pt(1B)–S(1B)	167.36(7)	P(2B)–Pt(1B)–S(2B)	86.85(7)	P(2B)–Pt(1B)–S(1B)	171.72(6)	P(2B)–Pt(1B)–S(2B)	89.78(6)
P(2B)–Pt(1B)–P(1B)	99.18(8)	S(2B)–Pt(1B)–S(1B)	80.54(6)	P(2B)–Pt(1B)–P(1B)	100.42(7)	S(2B)–Pt(1B)–S(1B)	81.96(5)
P(3B)–Pt(2B)–S(1B)	170.68(7)	P(3B)–Pt(2B)–S(2B)	90.44(7)	P(3B)–Pt(2B)–S(1B)	167.84(6)	P(3B)–Pt(2B)–S(2B)	85.81(6)
P(4B)–Pt(2B)–P(3B)	100.35(8)	P(4B)–Pt(2B)–S(2B)	168.31(7)	P(4B)–Pt(2B)–P(3B)	99.46(7)	P(4B)–Pt(2B)–S(2B)	174.40(6)
P(4B)–Pt(2B)–S(1B)	88.97(7)	S(1B)–Pt(2B)–S(2B)	80.26(6)	P(4B)–Pt(2B)–S(1B)	92.70(6)	S(1B)–Pt(2B)–S(2B)	82.05(5)
N(1B)–Zn(1B)–S(1B)	95.55(19)	N(1B)–Zn(1B)–S(2B)	136.2(2)	N(1B)–Cd(1B)–S(1B)	149.13(17)	N(1B)–Cd(1B)–S(2B)	95.08(17)
N(2B)–Zn(1B)–S(1B)	153.3(2)	N(2B)–Zn(1B)–S(2B)	93.6(2)	N(2B)–Cd(1B)–S(1B)	97.25(16)	N(2B)–Cd(1B)–S(2B)	131.44(17)
N(1B)–Zn(1B)–Cl(1B)	103.4(2)	N(2B)–Zn(1B)–Cl(1B)	95.8(2)	N(1B)–Cd(1B)–Cl(1B)	94.65(17)	N(2B)–Cd(1B)–Cl(1B)	104.05(17)
N(1B)–Zn(1B)–N(2B)	75.6(3)	S(1B)–Zn(1B)–S(2B)	75.32(6)	N(2B)–Cd(1B)–N(1B)	69.6(2)	S(1B)–Cd(1B)–S(2B)	72.40(5)
Cl(1B)–Zn(1B)–S(1B)	110.78(8)	Cl(1B)–Zn(1B)–S(2B)	120.04(8)	Cl(1B)–Cd(1B)–S(1B)	115.90(7)	Cl(1B)–Cd(1B)–S(2B)	123.42(7)

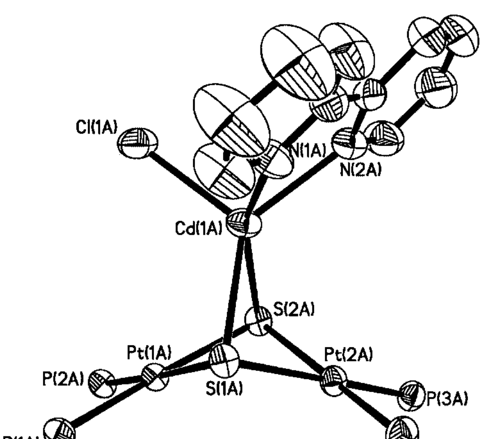

Fig. 2 Thermal ellipsoid plot (50% probability) of one of the two crystallographically independent molecules (A) of $[Pt_2CdCl(bipy)(PPh_3)_4(\mu_3\text{-}S)_2]^+$ (**3**) (phenyl rings are omitted for clarity).

cantly different in length (2.450(2), 2.533(2) and 2.565(2), 2.426(2) Å).

The Cd(II) analogue, $[Pt_2CdCl(bipy)(PPh_3)_4(\mu_3\text{-}S)_2][PF_6]$ (**3**) was prepared similarly. X-Ray analysis gave an isostructural $\{CdPt_2S_2\}$ complex (Fig. 2 and Table 1). The Cd(II) center also gives a sbp geometry with the Cd atom close to (0.60 Å) the basal plane. Unlike in **2**, the metalloligand is virtually symmetrically disposed on the Cd(II) center (Cd–S 2.627(2), 2.625(2) and 2.656(2), 2.586(2) Å), probably a result of less steric hindrance imposed on the bigger Cd(II). The sbp geometry contrasts the tbp structure found in $[CdCl_3(thiamin)]_2\cdot 2H_2O$ and $[CdCl_5]^{3-}$.[12]

The sbp structure in **2** and **3** is supported not by a macrocyclic ligand, but by two bidentate chelating ligands on its base. The usual tetrahedral geometry is probably not tolerable by the acute bite/chelate angles of both ligands (mean S–Zn–S 75.3°, N–Zn–N 74.8° and S–Cd–S 72.2°, N–Cd–N 69.1°) which are substantially smaller than a typical tetrahedral angle. As evidenced here and in the adduct $[InPt_2Cl_3(PPh_3)_4(\mu_3\text{-}S)_2]$,[13] **1** preferentially supports a sbp geometry despite the preference of the metal for tbp (or T_d). This illustrates the ability of complex **1** to stabilize an unusual coordination geometry of a metal.

With three different ligands on a metal with a distorted sbp structure, complex **2** would show four inequivalent phosphines in a static structure. This is inconsistent with the single resonance (δ 19.5) observed in the rt $^{31}P\text{-}\{^1H\}$ NMR spectrum of **2** in CD_2Cl_2. However, peak broadening occurs as the temperature is lowered and two distinct resonances (δ 20.1 and 17.5) eventually emerge at 243 K. These peaks broaden as the temperature decreases further, finally giving rise to four broad peaks (δ 21.8, 19.7, 15.9 and 12.9) at 183 K (Fig. 3). Similar behavior is observed for **3**, in which case the singlet (δ 20.6) at rt splits at 233 K into two discrete signals (δ 20.8 and 18.0) which broaden at lower temperatures. A Berry pseudorotation process whereby the axial chloride migrates from above to below the plane (Scheme 1) would account for the single resonance through rapid ligand interchanges. The registered energy barrier ($\Delta G^{\ddagger}$ = 51 kJ mol^{-1}) is significantly higher than that of a typical Berry rotation process because the mobility of the two bidentate ligands are restricted by their correlated movement which is limited by their acceptable chelate bite angles. A related fluxional process is found in a similar sbp complex $[NiL^1L^2]$-$(ClO_4)_2$ [L^1 = bis(2-(dimethylarsino)phenyl)methylarsine; L^2 = 1,2-phenylenebis(dimethylarsine)] which is reported to have a higher energy barrier ($\Delta G^{\ddagger}$ = 65.8 kJ mol^{-1}).[14] At 243 K, scrambling of the ligands in **2** and **3** is sufficiently slow to allow a sbp structure to be observed. Such a structure is however not static—the two sulfur donor atoms continue to flip up and down across the basal plane (Scheme 2). This is reminiscent of an exchange process between two sbp forms *via* a tbp transition state in a similar Ni(II) complex.[14] The equilibrium structure represents a regular sbp with a mirror plane comprising the Cl and three metal atoms. Such a structure would give two inequivalent pairs of phosphines on either side of the basal plane, which is consistent with the two distinct peaks observed. At 183 K, this motion is frozen to give an irregular sbp as observed in the crystal structure. In the absence of any symmetry, all the phosphines are inequivalent, as evidenced by the four discrete peaks in the NMR spectrum. An alternative fluxional model through chloride dissociation is dismissed as it would not support these spectral changes (see also below). The fluxional behavior of **3** can be described similarly.

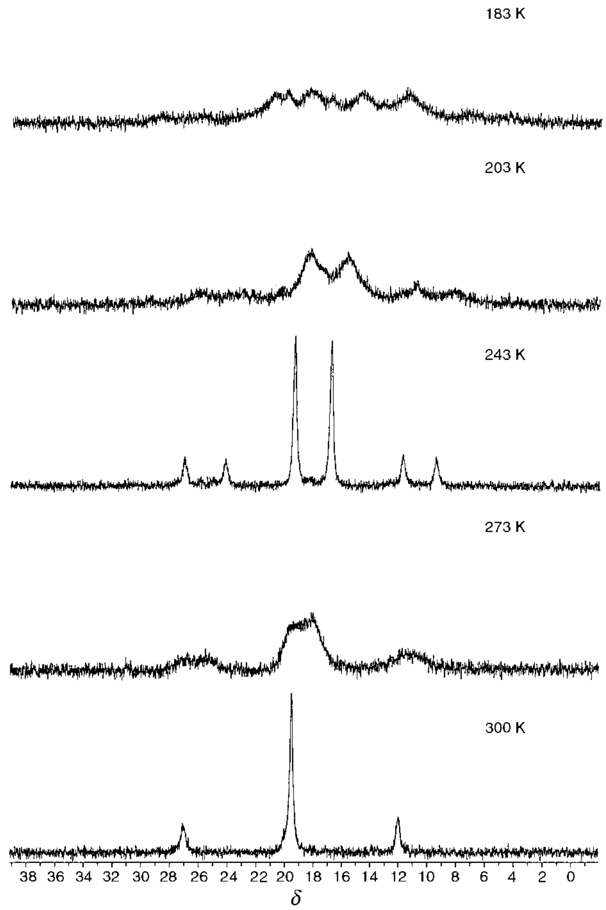

Fig. 3 VT-$^{31}P\{^1H\}$ NMR spectra of $[Pt_2ZnCl(bipy)(PPh_3)_4(\mu_3\text{-}S)_2]$-$[PF_6]$ (**2**) in CD_2Cl_2.

Electrospray ionization mass spectrometric (ESMS) analysis of **2** and **3** give the molecular peaks at *m*/*z* 1759.3 and 1806.4 respectively at a low cone voltage (5 V). Some ionization-induced fragmentations are also observed, leading to $[Pt_2S_2$-$(PPh_3)_4H]^+$ (*m*/*z* 1503.3) and $[Pt_2S_2(PPh_3)_4Zn(bipy)]^{2+}$ (*m*/*z* 861.2) in **2** and $[Pt_2S_2(PPh_3)_4H]^+$ (*m*/*z* 1503.3) in **3**.

Nonlocal density functional theory calculations reveal that for both **2** and **3**, the formation of the tbp intermediate is favoured over that of the tetrahedral species by 359.49 and 190.98 kJ mol^{-1}, respectively.[15] The optimized geometries of the

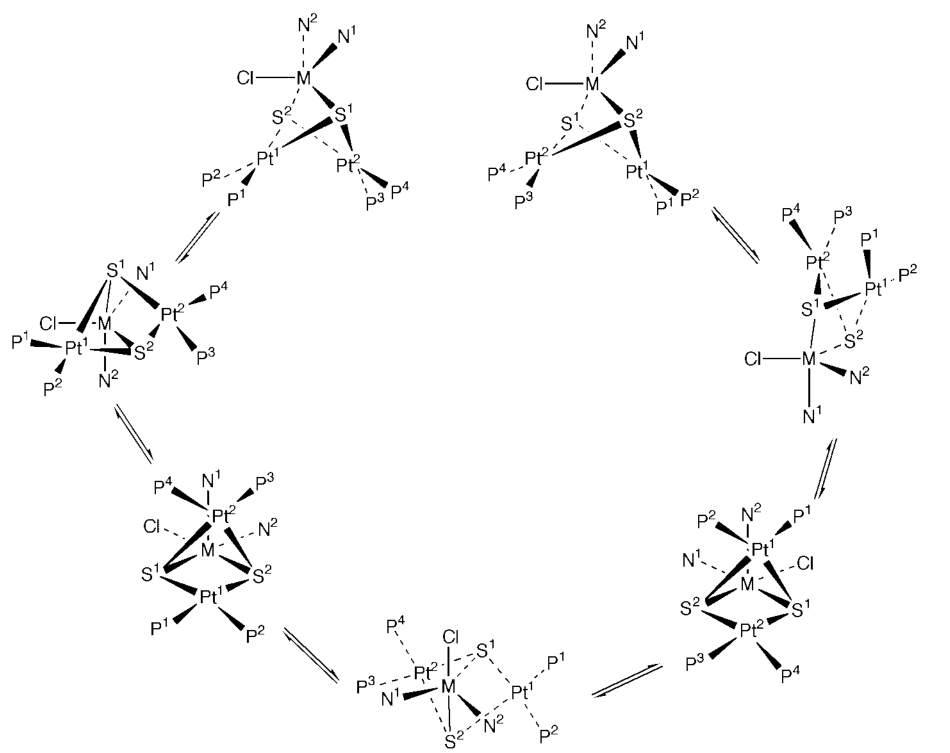

Scheme 1 Rapid ligand interchanges through a Berry pseudorotation, resulting in an "inversion" of the M–Cl bond from above to below the basal plane in a sbp structure.

Table 2 Optimized L–M–L bond angles for the T_d species

	M = Zn	M = Cd
N–M–N	80.7	73.9
S–M–S	81.3	75.9

Table 3 Calculated Mülliken overlap populations for the sbp species

	M = Zn	M = Cd
M–N	0.217, 0.188	0.160, 0.184
M–S	0.202, 0.271	0.162, 0.187
M–Cl	0.832	0.715

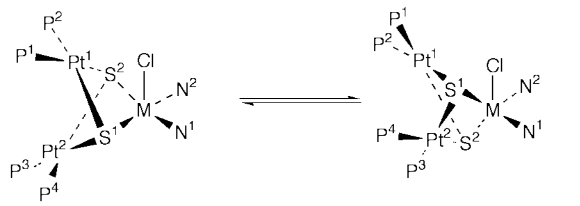

Scheme 2 A flipping or "fidgeting" movement of the $\{Pt_2S_2\}$ ligand across the basal plane of a sbp structure.

T_d species reveal L–M–L angles (M = Zn, Cd; L = N, S) with large deviations from the ideal T_d angle of 109.5° (Table 2). Mülliken overlap population analyses show that in comparison with the M–N and M–S bonds, the M–Cl bonds in the sbp structures are remarkably strong (Table 3). These could explain the preference for **2** and **3** to undergo a non-dissociative exchange over a dissociative T_d-type intermediate. We also found that the displacement of chloride in the sbp structure by a MeOH molecule is energetically unfavorable (ΔH = 655.24 kJ mol^{-1} for **2** and 658.00 kJ mol^{-1} for **3**);[16] this result further suggests that chloride dissociation is strongly suppressed even in the presence of a coordinating solvent. The experimental conductivity data of **2** and **3** also relate more to a 1 : 1 than a 2 : 1 electrolyte system. This unexpected strength of the M–Cl bond, which is also supported by the crystallographic data, underpins the stability of these 5-coordinated structures.

Experimental

All reactions were routinely performed under a pure argon atmosphere unless otherwise stated. All solvents were distilled and degassed before use. Complex **1** $[Pt_2(PPh_3)_4(\mu\text{-}S)_2]$ was synthesized from *cis*-$[PtCl_2(PPh_3)_2]$ and $Na_2S\cdot 9H_2O$ according to a literature method.[17] Elemental analyses were conducted in the Elemental Analysis Laboratory in the Department of Chemistry. The ^{31}P-$\{^1H\}$ NMR spectra were recorded on a Bruker ACF 300 spectrometer with H_3PO_4 as external reference. $\Delta G^\ddagger$ was experimentally determined from the coalescence temperature obtained in the VT spectra. The electrospray mass spectra were obtained in the positive-ion mode with a VG Platform II quadrupole mass spectrometer using HPLC-grade MeOH as the mobile phase under a cone voltage of 5 V.

Synthesis

$[Pt_2ZnCl(bipy)(PPh_3)_4(\mu_3\text{-}S)_2][PF_6]$ (2). A suspension of **1** (0.15 g, 0.1 mmol) and $ZnCl_2$ (0.014 g, 0.1 mmol) was stirred in MeOH (30 cm^3) for 6 h, and then bipy (0.016 g, 0.1 mmol) was added. The suspension changed to a clear bright yellow solution within a few min. The solution was filtered and purified by metathesis with NH_4PF_6 to yield complex **2**. The product was recrystallized in a CH_2Cl_2–MeOH (1 : 3) mixture to give yellow crystals (yield: 0.079 g, 54%). Anal. Calc. for $C_{82}H_{68}ClF_6N_2P_5Pt_2S_2Zn$: C, 51.65; H, 3.57; Cl, 1.81; F, 5.98; N, 1.47; P, 8.13; S, 3.36%. Found: C, 52.01; H, 3.04; Cl, 1.70; F, 5.88; N, 1.54; P, 8.54; S, 3.04%. ESMS (cone voltage 5 V): *m*/*z* = 1759.3 [20%, $[Pt_2S_2(PPh_3)_4Zn(bipy)Cl]^+$], 1503.3 [100%, $[Pt_2S_2(PPh_3)_4H]^+$], 861.2 [78%, $[Pt_2S_2(PPh_3)_4Zn(bipy)]^{2+}$]. ^{31}P-$\{^1H\}$ NMR (298 K, CD_2Cl_2): δ 19.5 [^1J(P-Pt) 3080 Hz]. IR (cm^{-1}): 840 (PF_6^-). Molar conductivity Λ_m (CH_2Cl_2, 10^{-3} M): 76.5 Ω^{-1} cm^2 mol^{-1}.

$[Pt_2CdCl(bipy)(PPh_3)_4(\mu_3\text{-}S)_2][PF_6]$ (3). Complex **3** was synthesized in a manner analogous to that of **2** by using **1** (0.15 g, 0.1 mmol), $CdCl_2$ (0.021 g, 0.1 mmol) and bipy (0.016 g, 0.1 mmol) in MeOH (30 cm^3). The resultant yellow solution was filtered and purified by metathesis with NH_4PF_6 to yield **3**. The product was recrystallized in a CH_2Cl_2–MeOH (1 : 3) mixture to give yellow crystals (yield: 0.069 g, 44%). Anal. Calc. for $C_{82}H_{68}CdClF_6N_2P_5Pt_2S_2$: C, 50.40; H, 3.48; Cl, 1.79; F, 5.84; N, 1.43; P, 7.94; S, 3.28%. Found: C, 50.92; H, 3.29; Cl, 1.61; F, 5.64; N, 1.29; P, 7.63; S, 3.14%. ESMS (cone voltage 5 V): *m*/*z* = 1806.4 [100%, $[Pt_2S_2(PPh_3)_4Cd(bipy)Cl]^+$], 1503.3 [40%, $[Pt_2S_2(PPh_3)_4H]^+$]. ^{31}P-$\{^1H\}$ NMR (298 K, CD_2Cl_2): δ 20.6 [^1J(P-Pt) 3002 Hz]. IR (cm^{-1}): 840 (PF_6^-). Molar conductivity Λ_m (CH_2Cl_2, 10^{-3} M) 77.7 Ω^{-1} cm^2 mol^{-1}.

Crystallography

Single crystals of **2** and **3** suitable for X-ray diffraction studies were grown from CH_2Cl_2–MeOH (1 : 3) by slow evaporation at rt in air. The crystals rapidly turned opaque upon isolation and were hence sealed in a quartz capillary with the mother liquor during data collection. Data collections of two crystals were carried out on a Siemens CCD SMART system at 293 K. Details of crystal and data collection parameters are summarized in Table 4.

The structures of the two complexes were solved by direct methods and difference Fourier maps. No solvate molecules were apparent. Full-matrix least-squares refinements were carried out with anisotropic thermal parameters for all non-hydrogen atoms except for fluorine atoms which were refined isotropically. Hydrogen atoms were placed on calculated positions (C–H 0.96 Å) and assigned isotropic thermal parameters riding on their parent atoms. Initial calculations were carried out on a PC using SHELXTL PC[18] software package; SHELXL-93[19] was used for the final refinements. Corrections for absorption were carried out by the SADABS method.[20]

CCDC reference number 186/1854.

See http://www.rsc.org/suppdata/dt/a9/a909254d/ for crystallographic files in .cif format.

Computational methods

Nonlocal density functional theory (NLDFT) calculations were carried out in GAUSSIAN 98.[21] Gradient corrections were introduced in a self-consistent manner by using the three-parameter hybrid exchange functional of Becke[22] (B3) and the correlation functional of Lee, Yang and Parr[23] (LYP). The LanL2DZ basis set was chosen for our calculations. This basis set consists of the Dunning–Huzinaga valence double-zeta basis[24] on H and C, and a combination of the quasi-relativistic LanL2 effective core potentials[25] and valence double-zeta[24] on all other atoms. Bond overlap populations were calculated by using Mülliken population analysis. The input structures for the sbp species were obtained from X-ray crystal structures. Geometry optimizations of the tbp species were carried out by constraining the metal center in an ideal tbp geometry. To simplify calculations, the phenyl rings on the phosphines were replaced with hydrogen atoms; the P–H bond length was set at the sum of covalent radii of P and H (1.42 Å).

Table 4 Crystallographic data and refinement details for $[Pt_2ZnCl(bipy)(PPh_3)_4(\mu_3\text{-}S)_2]^+$ (**2**) and $[Pt_2CdCl(bipy)(PPh_3)_4(\mu_3\text{-}S)_2]^+$ (**3**)

	2	**3**
Chemical formula	$C_{82}H_{68}ClF_6N_2P_5Pt_2S_2Zn$	$C_{82}H_{68}CdClF_6N_2P_5Pt_2S_2$
Formula weight	1905.35	1952.38
Crystal size/mm	0.45 × 0.30 × 0.13	0.45 × 0.30 × 0.10
Crystal system	Triclinic	Triclinic
Space group	$P\bar{1}$	$P\bar{1}$
a/Å	14.5319(2)	14.5256(5)
b/Å	20.0832(2)	20.1188(7)
c/Å	29.2213(3)	29.3002(11)
U/Å^3	8413.36(17)	8433.7(5)
α/°	83.434(1)	83.110(1)
β/°	88.522(1)	88.390(1)
γ/°	83.281(1)	82.842(1)
Z	4	4
μ/mm^{-1}	3.831	3.790
F(000)	3752	3824
θ range for data collection	1.58 to 26.33°	1.64 to 26.42°
No. of reflections collected	66741	67852
No. of unique data	33316	33714
No. of reflections [$I > 3\sigma(I)$]	24966	26677
Residuals: R_1, wR_2 (observed data)	0.0508, 0.1345	0.0417, 0.1191
Residuals: R_1, wR_2 (all data)	0.0753, 0.1477	0.0592, 0.1301
Goodness of fit	1.054	1.084

Acknowledgements

The authors acknowledge the National University of Singapore (NUS) for financial support. Z. L. thanks NUS for a research scholarship award. Technical support from the Department of Chemistry of NUS is appreciated.

References

1 R. A. Santos, E. S. Gruff, S. A. Koch and G. S. Harbison, *J. Am. Chem. Soc.*, 1991, **113**, 469.
2 R. T. Dworschach and B. V. Plapp, *Biochemistry*, 1977, **16**, 2716.
3 M. Melnik, *J. Coord. Chem.*, 1995, **35**, 179.
4 L. D. Spaulding, L. C. Andrews and G. J. B. Williams, *J. Am. Chem. Soc.*, 1977, **99**, 6918.
5 N. W. Alcock, N. Herron and P. Moore, *J. Chem. Soc.*, *Dalton Trans.*, 1978, 1282.
6 M. C. R. Arguelles, L. P. Battaglia, M. B. Ferrari, G. G. Fava, C. Pelizzi and G. Pelosi, *J. Chem. Soc.*, *Dalton Trans.*, 1995, 2297.
7 H. Strasdeit, W. Saak, S. Pohl, W. L. Driessen and J. Reedijk, *Inorg. Chem.*, 1988, **27**, 1557.
8 G. V. Long, S. E. Boyd, M. M. Harding, I. E. Buys and T. W. Hambley, *J. Chem. Soc.*, *Dalton Trans.*, 1993, 3175.
9 J. S. Casas, E. E. Castellano, M. D. Couce, A. Sanchez, J. Sordo, J. M. Varda and J. Z. Schpector, *Inorg. Chem.*, 1995, **34**, 2430.
10 S. W. A. Fong and T. S. A. Hor, *J. Chem. Soc.*, *Dalton Trans.*, 1999, 639 and refs therein; T. S. A. Hor, *J. Cluster Sci.*, 1996, **7**, 262 and refs. therein.
11 C. Zhang, R. Chadha, H. K. Reddy and G. N. Schrauzer, *Inorg. Chem.*, 1991, **30**, 3865.
12 E. F. Epstein and I. Bernal, *J. Chem. Soc. A*, 1971, 3628.
13 M. S. Zhou, Y. Xu, C. F. Lam, P. H. Leung, L. L. Koh, K. F. Mok and T. S. A. Hor, *Inorg. Chem.*, 1994, **33**, 1572.
14 M. G. Fitzpatrick, L. R. Hanton and D. A. McMorran, *Inorg. Chem.*, 1995, **34**, 4821.
15 We noted that a rigorous theoretical treatment of fluxional behavior requires the geometries and energies of the respective transition states to be computed. However, such calculations were omitted in this study because the energetic requirements for the formation of the tbp species were found to be much smaller than those required for the formation of the T_d species. Hence, we believe that the difference in kinetic preferences of the two fluxional processes can be easily overcome by the strong thermodynamic preference for the tbp species.
16 The position of the MeOH molecule was fixed such that the M–O bond lengths (M = Zn, Cd) correspond to the sum of covalent radii (Zn–O 2.090 Å, Cd–O 2.318 Å).
17 R. Ugo, G. La Monica, S. Cenimi, A. Segre and F. Conti, *J. Chem. Soc. A*, 1971, 522.
18 G. M. Sheldrick, SHELXTL-PC, release 4.4, Siemens Analytical X-Ray Instruments, Madison, W1, 1992.
19 G. M. Sheldrick, SHELXL-93, *Program for Crystal Structure Refinement*, University of Göttingen, Germany, 1993.
20 G. M. Sheldrick, SADABS, Program for Siemens area detector absorption correction, University of Göttingen, Germany, 1996.
21 GAUSSIAN 98 (Revision A.7), M. J. Frisch, G. W. Trucks, H. B. Schlegel, G. E. Scuseria, M. A. Robb, J. R. Cheeseman, V. G. Zakrzewski, J. A. Montgomery, R. E. Stratmann, J. C. Burant, S. Dapprich, J. M. Millam, A. D. Daniels, K. N. Kudin, M. C. Strain, O. Farkas, J. Tomasi, V. Barone, M. Cossi, R. Cammi, B. Mennucci, C. Pomelli, C. Adamo, S. Clifford, J. Ochterski, G. A. Petersson, P. Y. Ayala, Q. Cui, K. Morokuma, D. K. Malick, A. D. Rabuck, K. Raghavachari, J. B. Foresman, J. Cioslowski, J. V. Ortiz, B. B. Stefanov, G. Liu, A. Liashenko, P. Piskorz, I. Komaromi, R. Gomperts, R. L. Martin, D. J. Fox, T. Keith, M. A. Al-Laham, C. Y. Peng, A. Nanayakkara, C. Gonzalez, M. Challacombe, P. M. W. Gill, B. G. Johnson, W. Chen, M. W. Wong, J. L. Andres, M. Head-Gordon, E. S. Replogle and J. A. Pople, Gaussian, Inc., Pittsburgh PA, 1998.
22 A. D. Becke, *J. Chem. Phys.*, 1993, **98**, 5648.
23 C. Lee, W. Yang and R. G. Parr, *Phys. Rev. B*, 1988, **37**, 785.
24 T. H. Dunning, Jr. and P. J. Hay, in *Modern Theoretical Chemistry*, ed. H. F. Schaeffer III, Plenum, New York, 1976, p. 1.
25 P. J. Hay and W. R. Wadt, *J. Chem. Phys.*, 1985, **82**, 270, 284; W. R. Wadt and P. J. Hay, *J. Chem. Phys.*, 1985, **82**, 299.

Paper a909254d